

Ethanol as a 'Catalyst' for Effective Phase Transfer and Self-Assembly of Gold Nanorods

Min Zhang,^[a] Tian-Song Deng,^{*,[a]} and Zhiqun Cheng^[a]

Transferring gold nanorods (GNRs) from an aqueous solution to a non-polar solvent enhances self-assembly, promotes biocompatibility, and boosts surface-enhanced Raman scattering (SERS). However, the strong attachment ability of toxic hexadecyltrimethylammonium bromide (CTAB) to GNRs presents a significant challenge in the fall of CTAB and combining with other substances for self-assembly and SERS applications. We propose a solution that employs ethanol as a 'catalyst' to lower the critical micelle concentration (CMC) of CTAB and efficiently combine it with the organosilanes formed

by the hydrolysis of mercaptopropyltrimethoxysilane (MPS) and octadecyltrimethoxysilane (ODS). The samples were characterized by UV-vis-NIR spectroscopy, transmission electron microscopy (TEM), and energy disperse spectroscopy (EDS) mapping. A detailed interpretation of the phase transfer processes was provided. The modified particles were effectively dispersed in toluene and formed thin films at the air-water interface through self-assembly, which was confirmed by scanning electron microscopy (SEM) and optical microscopy. These films can serve as a platform for SERS.

Introduction

Plasmonic nanoparticles have generated a tremendous interest owing to their appealing biocompatible,^[1] catalytic,^[2] electronic^[3] and optical properties,^[4] which allowed the exploitation of many applications.^[5] Among these, gold nanorods (GNRs) have gained prominence clearly due to their superior longitudinal plasmon resonances that strongly depend on the aspect ratio (length/diameter).^[6] The aspect ratio can be tuned facially from the visible to the (near-) infrared region,^[7] which are efficient for photothermal therapy, high photothermal conversion, and prolonging the half-life of blood circulation.^[8]

GNRs can be synthesized in both polar and non-polar environments, however it is important to ensure a meticulous preparation process in a polar environment, as the interaction between gold particle and water molecules is intense, leading to diminished functional properties.^[9] On the other hand, GNRs were synthesized in a non-polar environment are particularly challenging to control their shape and size, making them more sensitive. Additionally, without ligand binding, monolayers formed have a wider nanogap due to inherent van der Waals interactions of repulsion and mutual attraction between nanoparticles, which weakens surface-enhanced Raman scattering (SERS) enhancement.^[10] Therefore, effective phase transfer from a polar to a non-polar solvent is absolutely critical and requires two vital steps. The first step involves changing the ligands with higher affinity, commonly achieved using molecules with alkylamines groups^[11] or thiol functions.^[12] The second step involves promising that the replaced particles contain solvent-compat-

ible parts for sufficient solubility.^[13] Previous studies have typically focused on particles no larger than 20 nm in phase transfer methods,^[14] but there are now more efforts on the realization of phase transfer of larger particles.^[15] For instance, gold nanoparticles (>20 nm) were coated with polyoxyethylene alkyl amine surfactants (AMIETs) and transferred to chloroform. The isoelectric point was affected by adjusting the number of ethyleneoxy units, which altered the solution's pH value. AMIETs are mixtures of polyoxyethylene alkyl amines.^[16] The combination of the thiol functional group and the metal surface forms a loose monolayer on the nanoparticle surface, allowing for efficient dissolution by organic solvent molecules without a sudden change in refractive index.^[13b] However, the process of phase transfer using amphiphilic polymers to study biocompatibility of polymer-coated gold NPs in different cell lines is time-consuming. It takes 4 days for GNRs and a minimum of 12 hours for other particles.^[17] Derikov et al. effectively prepared hybrid composites utilizing a high molecular mass block copolymer of styrene and 2-vinylpyridine to exchange ligands on the surface of gold nanoparticles, without the need for strong thiol and amine surfactants. This method resulted in transmission micrographs with significantly much impurities and poor monodispersity.^[18]

In addition, it is difficult for the particles at the water-oil interface to form a stable structure, unlike their air-water interface counterparts, which can occur after phase transfer. Modifying particle size to enhance ionic activity can effectively produce materials with SERS enhancement, and its structure is ideal for creating uniformly stable substrates.^[19] Liz-Marzan et al. and Kotkowiak et al. effectively diffused organic dispersions in water and employed the Langmuir-Blodgett technique to assemble nanoparticles into ordered arrays at the air-water interface, which can then be transferred to solid substrates with ease. The dense arrangement of nanoparticle arrays results in significant plasmonic coupling, creating a valuable substrate for SERS spectroscopy.^[20] However, the process of forming a film

[a] M. Zhang, Prof. Dr. T.-S. Deng, Prof. Dr. Z. Cheng
School of Electronics and Information Engineering, Hangzhou Dianzi
University, Hangzhou 310018, P. R. China
E-mail: dengts@pku.edu.cn

Supporting information for this article is available on the WWW under
<https://doi.org/10.1002/slct.202301065>

from these particles can be complicated. To develop a stable and simple platform for subsequent preparation of GNRs, it is crucial to identify the most suitable ligand for their surface. Finding a strong driving force for successful ligand exchange remains a challenge.

Here, we have developed an effective and reliable method for transferring GNRs from an aqueous solution into a non-polar solvent. The modified GNRs can be self-assembled into a film suitable for a SERS platform. Our methodology, which involves the use of ethanol as a 'catalyst', facilitates the combination of GNRs with organosilanes resulting in a hydrophobic surface, resulting the dispersion of GNRs in non-polar solvents like toluene. This surface modification technique can be extended to other nanoparticles, including gold nanospheres (GNPs), effectively between phases.

Results and Discussion

The successful phase transfer of GNRs was achieved by treating of hexadecyltrimethylammonium bromide (CTAB)-capped GNRs in a two-phase system (water and toluene). Figure 1 depicts the scheme of the phase transfer process. The process of CTAB-

capped GNRs transforming into mercaptopropyltrimethoxysilane-octadecyltrimethoxysilane-capped (MPS-ODS-capped) GNRs involves three steps: (i) combining GNRs with hydrolyzed MPS (Si-OR) after the ligand CTAB is removed with ethanol, (ii) hydrolyzing ODS in sodium hydroxide solution (Si-OR) and (iii) immobilizing the two hydrolyzed products undergo condensation reaction to form hydrophobic organosilanes on the GNRs (Figure 1a). Through the three steps, the CTAB-capped GNRs could be modified into GNRs coated with hydrophobic organosilanol shell, which stabilizes them in toluene solution. Figure 1b illustrates the change of surfactant ligands on the surface of GNRs in the solution.

After synthesizing the GNRs through the seed-mediated method and dispersing them in water, the MPS-ODS-capped GNRs were obtained by undergoing ligand exchange via centrifugation and washing. The efficiency of phase transfer is relatively high, as only a small fraction of particles remained in the aqueous phase or water-toluene interface. In Figure 2a, the extinction spectra of the modified GNRs show no significant changes compared to the original spectra. The LSPR peak has redshifted by 45 nm after surface modification, which attributes to the increase in refractive index of the solution and the formation of synthetic organosilane^[21] after surface modification

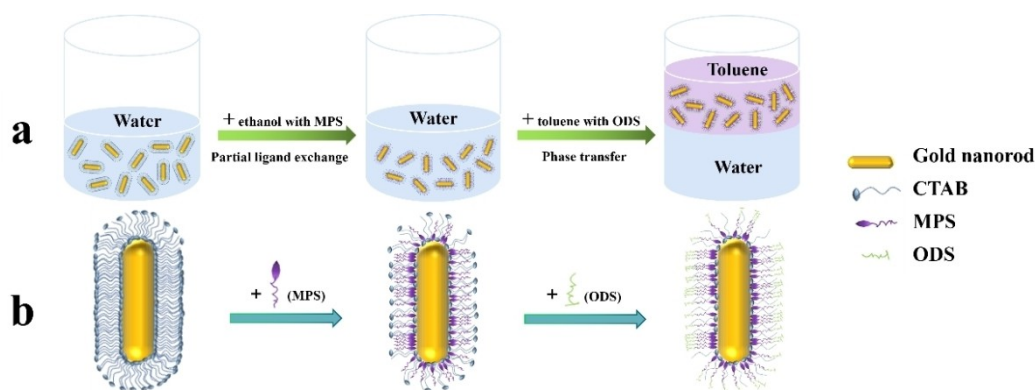


Figure 1. Depicting the phase transfer process of GNRs. (a) A step-by-step illustration of the experimental procedures, and (b) a representative schematic of the ligand transformation occurring on the GNRs' surface throughout the experiment.

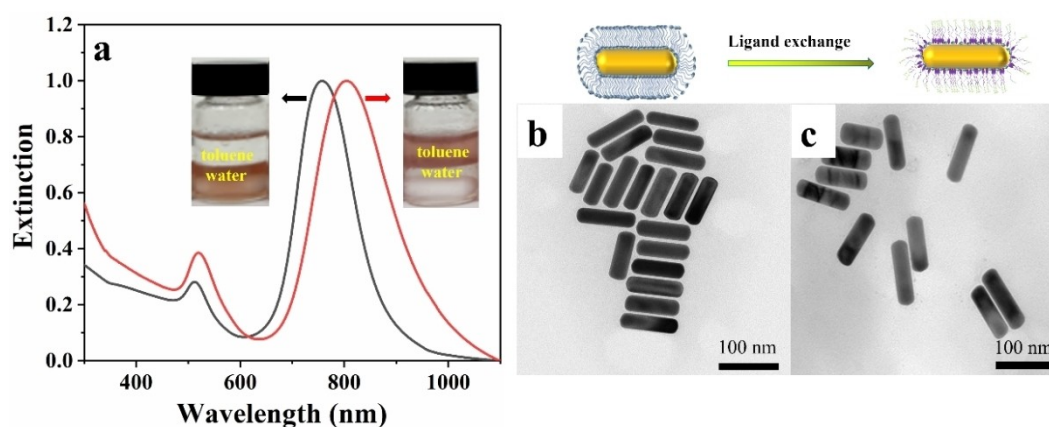


Figure 2. (a) Extinction spectra of GNRs both before and after the ligand exchange. Insets of (a) showing the optical images of solution before and after the ligand exchange. Representative transmission electron microscopy (TEM) images of GNRs before (b) and after (c) ligand exchange, respectively. The aspect ratio of the GNRs were 3.2 ± 0.4 and 3.2 ± 0.3 , respectively.

of GNRs. To further expand the variety of solvents in which the stable dispersions of modified GNRs can be obtained, we observed in Figure S1 that the modified GNRs exhibited purplish-red dispersion in THF because it is an aprotic polar solvent. Additionally, the modified GNRs can stable in chloroform with excellent solubility. The synthesized CTAB-capped (Figure 2b) and MPS-ODS-capped (Figure 2c) nanoparticles were analyzed by TEM images, which was observed the morphology of nanoparticle in a nonpolar solution without any noticeable changes. As an example of extensive application, GNRs exhibited a relatively regular shape and the particles size of 66.1 ± 8.2 nm (Figure S2) were modified by this method. As shown in Figure S3a, the GNRs were transferred from the aqueous phase to toluene phase following the same process. Furthermore, the extinction spectra before and after the modification were compared in Figure S3b, indicating that the peak value had redshifted because of an increase in the refractive index and changes in the dielectric constant around the GNRs in the solution.

To characterize the surface ligand composition of the modified GNRs, energy disperse spectroscopy (EDS) mapping

was performed. Figure 3 shows the high-angle annular dark-field scanning transmission electron microscopy (HAADF-STEM) image (Figure 3a) and the related elemental mapping images (Figure 3b) of Au (blue), Si (red), and S (green), respectively. Visualization of the relative distribution of Si and S elements confirms the well-modified results by MPS and ODS, as both compounds contain silicon and sulfur elements resulting from their hydrolysis.

Precise conditions for phase transfer are crucial for self-assembly and SERS. Systematic experiments on the amount of ethanol were performed. Obviously, it was evident that the spectra had the narrowest full wavelength at half maximum (FWHM) (Figure 4a) and the highest intensity when 100 μ L of ethanol was used (Figure 4b). This indicated that the transfer yield was ideal. Under other conditions, the nanoparticles either remained in water or agglomerated. The addition of an appropriate amount of ethanol was necessary to effectively reduce the critical micelle concentration (CMC) of CTAB for GNRs and help them firmly combine with MPS. Therefore, ethanol played a significant role in the process of ligand exchange. Under low concentration of ethanol (50 μ L), GNRs are

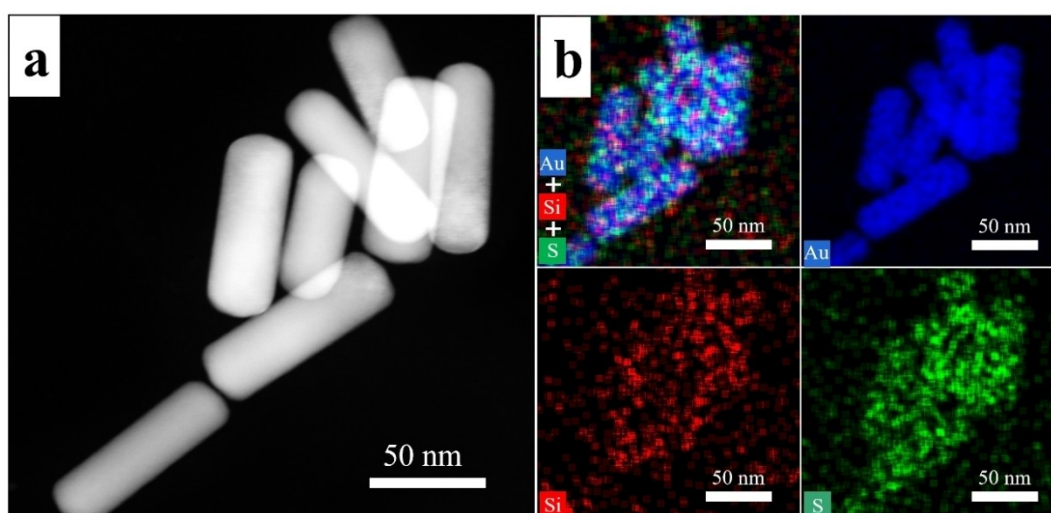


Figure 3. (a) Representative HAADF-STEM image and (b) elemental mapping images of Au (blue), Si (red), and S (green) of GNRs after surface modification.

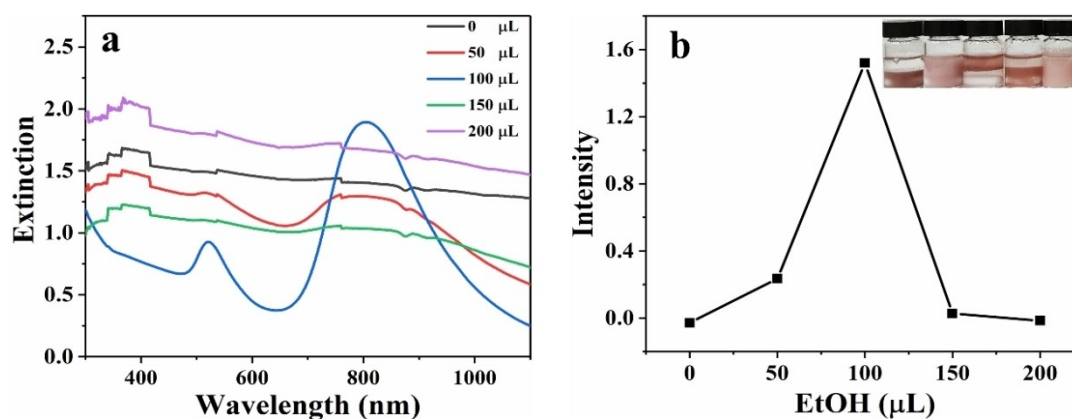


Figure 4. (a) Extinction spectra of different ethanol contents and (b) extinction intensity of different ethanol content. Insets of (b) showing the optical image of ligand modification.

stable with a CTAB bilayer. Increasing the concentration of ethanol can dissolve more of the bilayer, leading to an unbalanced state for the GNRs as a single hydrophobic layer gradually forms. Further increase in ethanol concentration causes the CTAB's hydrophobic layer to extend from the surface of the GNRs and became too firm to easily combine with other hydrophobic substances. However, if ethanol concentration continues to rise, irreversible aggregation may equally occur.^[22] Careful control of the amount of ethanol used throughout the surface modification process is crucial. Ethanol acts as a 'catalyst' by promoting ligand exchange, aiding in solubilization, and ensuring the solution stability after silane hydrolysis. Silane alcohol aqueous solution exhibits superior stability compared to silane aqueous solution, facilitating a smooth phase transfer process. The effects of MPS (Figure S4) and NaOH (Figure S5) were also tested with small amounts resulting in slow particle modification and weak hydrolysis, while excessive amounts led to greater degree of hydrolysis in organic matter, promoting easier connection between hydroxyl groups and resulting in particle agglomeration following hydrolysis.

To understand the mechanism of the phase transfer process, we proposed the following explanation. In an aqueous alcohol solution, the hydrolysis of MPS can be represented by scheme 1.

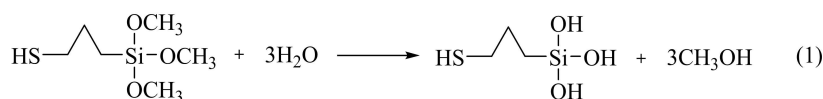
ODS is insoluble in aqueous solution, making it arduous to hydrolyze. However, the addition of sodium hydroxide facilitates the hydrolysis and subsequent combination with MPS. The existence of OH⁻ and H⁺ are indispensable for the hydrophobation of GNRs. It is important to note that OH⁻ has a stronger degree of hydrolysis compared to H⁺, which is attributed to the distinct catalytic effect under alkaline and acidic conditions.^[23] Scheme 2 shows the hydrolysis process of ODS.

Subsequently, as shown in scheme 3, the solution retains the alkaline catalyst required for efficient reaction between the hydrolysate of MPS and ODS, resulting in the formation of a stable Si–O–Si bond. Organosilane was formed by the combination of the MPS and ODS, which is then coupled to the surface

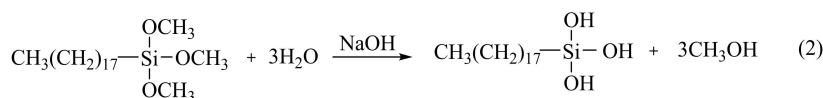
of GNRs through Au–S covalent bonding, thereby increasing their stability in toluene solution.

Plasmonic coupling has been demonstrated as an effective means of assessing the plasmonic properties of high-quality SERS signals.^[24] It is worth noting that these molecular films have several advantages in the fabrication of SERS substrates. For instance, achieving a uniform and sizeable area in the square centimeter range avoids the occurrence of "coffee ring" or similar local effects. Therefore, an even and dense molecular layer can be easily created using a simple experimental technique involving phase transfer and assembly, which can be scaled up to any larger surface area with the appropriate adjustment of nanoparticles quantities. The process of fabricating a molecular film was shown in Figure 5a. GNRs solution is added dropwise at the air-water interface, forming a densely packed film once the organic solvent volatilization. The assembled film was transferred on a silicon wafer (5 mm × 5 mm) is displayed in Figure 5b, while Figure 5c demonstrates its optical microscopic images, revealing a uniform film. To investigate the internal structure of the film, SEM image using acetone-cleaned silicon as the substrate was utilized as displayed in Figure 5d. Patel et al. has proposed that an appropriate concentration of micelles leads to a fine structural in the film, ultimately resulting in terrific stability.^[25]

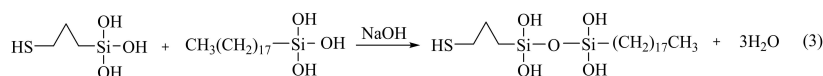
SERS detection is a powerful and ingenious analytical technique that enable the understanding of the function for molecules absorbed onto GNRs films and effects of concentration on SERS. Under the laser excitation of 785 nm, different concentrations of R6G probe molecule ranging from 10⁻⁵ M to 10⁻³ M were deposited on both the modified GNRs films-based SERS detection substrate and without GNRs films-based SERS detection substrate. As indicated in Figure 6, compared to the GNRs films, the Raman signal of the R6G solution alone was significantly weakened. Notably, at the concentration of 10⁻⁵ M and 10⁻³ M, significant vibrational bands was displayed, including broad bands around 1310 cm⁻¹ attributed to the stretching vibration of C=C, Raman peak at 1364 and 1509 cm⁻¹ attributed to the stretching vibration of C–C, a Raman peak at 1574 cm⁻¹



Scheme 1. The hydrolysis process of MPS.



Scheme 2. The hydrolysis process of ODS.



Scheme 3. The hydrolyzed MPS and ODS are connected.

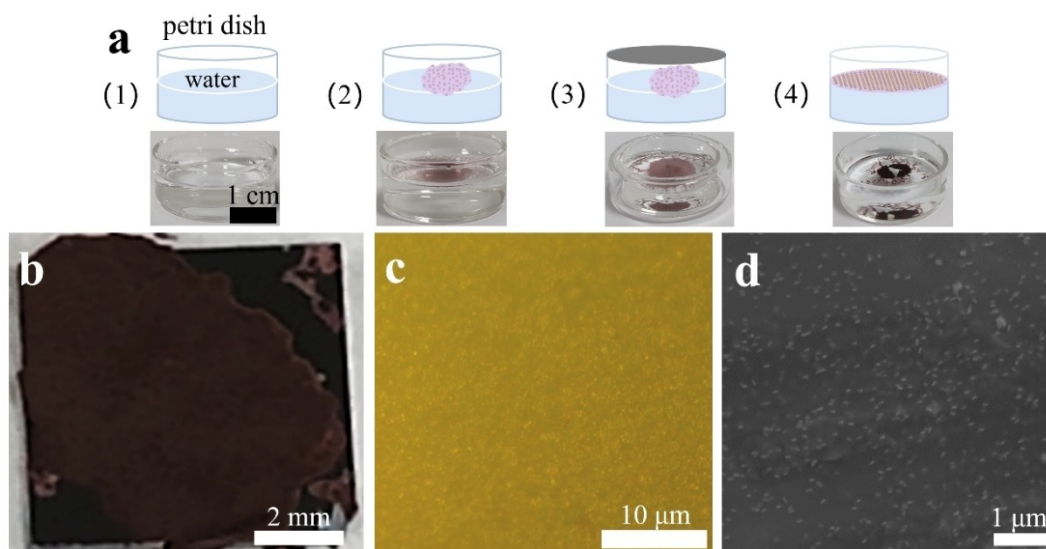


Figure 5. Fabrication and characterization of thin films. (a) The formation process of thin film. (b) The thin film is placed on a silicon wafer. (c) The microscope image of the thin films. (d) SEM image of thin films.

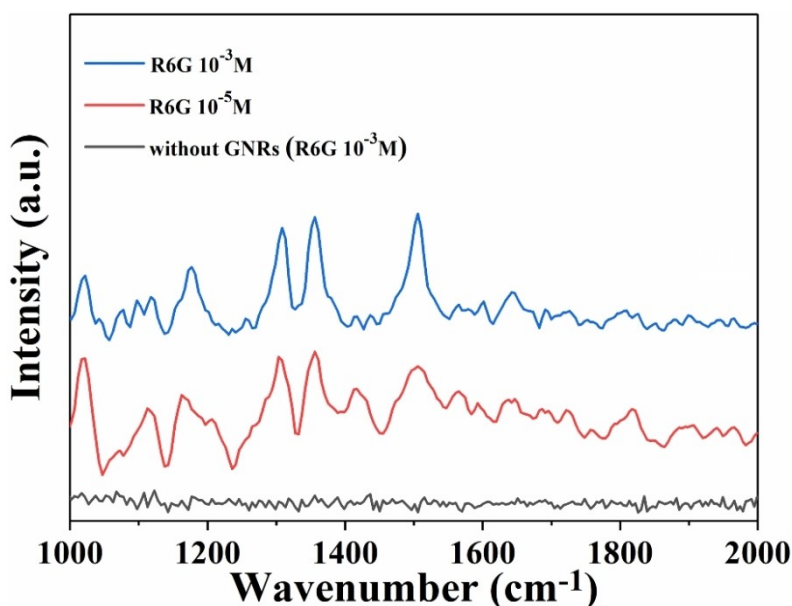


Figure 6. SERS spectra of R6G (ethanol) adsorbed on the films at different concentrations and without GNRs films. Experimental conditions are as follows: $\lambda_{\text{exc}} = 785 \text{ nm}$, power = 200 mW \times 70%, integration time = 10 s.

attributed to the stretching vibration of C=O, and an additional high signal around 1182 cm^{-1} attributed to C–H in-plane deformation vibration and N–H vibration of oxygen ring.^[26] The Raman intensity proportionally increases with the concentration of R6G due to increased number of scattering molecules and their larger surface area contact with the film. The results of SERS signal measurement are affected by several additional factors such as the adsorption capacity of different dyes, the presence of surfactants, contaminants, and surface defects.

Conclusions

In summary, the phase transfer technique described involves functionalizing the surface of GNRs with a mixture of hydrolyzing MPS and ODS, using ethanol as a ‘catalyst’. In order to facilitate transfer aqueous dispersions to toluene. The stability of the modified GNRs was confirmed by UV-vis spectra and TEM measurements. By introducing ethanol, the CTAB can be desorbed from the surface, leading to enhanced stability and exchange of GNRs. The three-step functionalization scheme maintains colloid stability while effectively balancing the removal of CTAB and the adhesion of MPS. Because of the

plasmonic coupling between particles, we analyzed the SERS activity of identical plasma substrate compositions produced with varying concentrations of R6G, and discovered superior SERS signal with higher concentration. It not only enhances comprehension of the phase transfer principle, but also promotes the advancement of NP self-assembly at the air-water interface in practical applications.

Experimental Section

Materials

All chemicals were obtained from commercial suppliers and used without further purification. Hexadecyltrimethylammonium bromide (CTAB, >99.0%) was purchased from TCI America. Chloroauric acid (HAuCl₄), L-ascorbic acid (AA, >99.99%), rhodamine 6G (R6G), hydrochloric acid (HCl, 37 wt.% in water), mercaptopropyltrimethoxysilane (MPS, 97%), poly (dimethyldiallylammonium chloride) (PDDA, Mw 400 000–500 000, 20 wt.% in H₂O), phosphoric acid (H₃PO₄, ≥85 wt.% in H₂O), ethylene glycol (EG, 98%) and methyl silicone oil were purchased from Shanghai Macklin Biochemical Technology Co., Ltd. Silver nitrate (AgNO₃, >99.8%), sodium oleate (NaOL, >99.88%), sodium borohydride (NaBH₄, >98%), octadecyltrimethoxysilane (ODS, 90%) and tetrahydrofuran (THF, 99.0%) were purchased from Shanghai Aladdin Biochemical Technology Co., Ltd. Sodium hydroxide (NaOH, >96%) was purchased from Hangzhou Gaojing Fine Chemical Industry Co., Ltd. Toluene (TOL, ≥99.5%) and chloroform were purchased from National Pharmaceutical Group Chemical Reagent Co., Ltd. Collective constant temperature heating magnetic agitator was purchased from Bangxi Instrument Technology (Shanghai) Co., Ltd. Ultrapure water (>18.2 MΩ) obtained from a Milli-Q water system was used in all experiments. All glassware were cleaned using freshly prepared aqua regia (HCl:HNO₃ in a 3:1 ratio by volume) followed by rinsing with copious amounts of water.

Synthesis of the Gold Nanostructure

GNRs (94 ± 9 nm in length; 29 ± 3 nm in width) of aqueous phase were synthesized in accordance with the mechanism of seed-mediated growth.^[27] Briefly, the seed solution was prepared by CTAB (10.0 mL, 0.1 M) solution mixed with HAuCl₄ (0.25 mL, 10.0 mM) solution in a 20 mL vial. Fresh NaBH₄ (0.6 mL, 0.01 M) solution was injected to the solution under vigorous stirring (1200 rpm). After stirring for 2 min and observing a color changed from yellow to brownish, the mixture was allowed to rest for 30 min before use. The growth solution was prepared by mixing CTAB (192.0 mL, 0.1 M) solution with NaOL (81.0 mL, 50.0 mM) and AgNO₃ (18.0 mL, 4 mM), which was kept undisturbed at 30 °C for 15 min. Afterwards, HAuCl₄ (25.0 mL, 10.0 mM) solution and 165.85 mL water were added. With the colorless solution, HCl (18.15 mL, 1.0 M) was added at low stirring at 400 rpm for 15 min. Finally, the AA (1.25 mL, 64 mM) and seed solution (0.8 mL) were added under vigorous stirring for 30 s and left undisturbed for 12 h. After being centrifuged at 7,000 rpm for 15 min, the solution was isolated and the supernatant was removed for twice. The GNRs (500 mL) were finally concentrated and redispersed in a CTAB solution (200 mL, 1.6 mM).

GNPs (66.1 ± 8.2 nm) was synthesized^[28] following a 20 mL EG solution was stirred at 600 rpm in a glass vial, and then 0.4 mL of PDDA and H₃PO₄ (0.8 mL, 1.0 M) were added in turn. The mixture was stirred for 2 min, and HAuCl₄ (0.02 mL, 0.5 M) was added under stirring which was maintained at the room temperature for 15 min,

and then the solution was bathed in an oil at 195 °C for 30 min. We centrifuged the solution at 12000 rpm and redispersed the precipitates in ethanol three times to remove the excess reactants and byproducts. The unwashed GNPs suspension was loaded into an oil bath at 195 °C for 1 h. The final solution was isolated by centrifugation at 12000 rpm for 15 min in ethanol and water for once. Similarly, GNPs were concentrated and redispersed in aqueous solution.

Phase Transfer Procedure of Gold Nanostructure

In a typical procedure, 1.0 mL aqueous nanoparticles were first mixed with MPS (0.02 mL, 10.0 mM) and 0.1 mL ethanol in a 5 mL vial under stirring at room temperature for 3 h. Concomitantly, 0.02 mL ODS solution was mixed with 1.5 mL toluene and NaOH (0.55 mL, 0.1 M) in a 5 mL vial under stirring at room temperature for 3 h. Phase transfer occurred after mixing the two solutions and stirring for 4 h. The organic solution was purified by centrifuging at 8000 rpm with ethanol for 5 min and washed with water for three times, and finally stored in toluene solution.

Dispersion of Modified GNRs in different solvents

Modified GNRs stock solution in toluene was purified by centrifuging at 8000 rpm for 5 min and dispersed in different solvents such as THF, chloroform and toluene. The same volume of water was added.

Self-assembly of Modified GNRs and Sample Preparation for SERS

Before using self-assembled thin film for SERS experiments. The silicon wafers were thoroughly cleaned by sonication in water with acetone for 5 min and then rinsed twice with ethanol, and placed in a 60 °C oven until the wafers were completely dried. The petri dish with a diameter of 3 cm was cleaned by ethanol and Milli-Q water, and was dried for 2 h at 60 °C. Dispersions of the ligand exchange solution in toluene were dropped on the surface of the petri dish with 4 mL of Milli-Q water. The petri dish is covered to prevent toluene from volatilizing too quickly and causing the film to disperse. After 1 h, it formed a homogeneous continuous film at the air-water interface. Thin films are deposited on silicon wafers as substrates and immediately incubated with 20 μL of a 1.0 mM R6G aqueous solution for 2 h at 60 °C.

Characterizations

All absorption measurements were captured on a UV-1900i spectrophotometer (SHIMADZU, Japan) with a 10.0 mm optical path, whereby a glass cuvette filled with Milli-Q water or toluene was used as the reference. Transmission electron microscopy (TEM) images were captured on a HT-7700 microscope (HITACHI, Japan) operating at 100.0 kV. Scanning electron microscopy (SEM) imaging was performed on an JEOL JSM6460-LV microscope operating at 3 kV. Energy dispersive spectroscopy (EDS) mapping were performed by a Fei-Talos-F200S operated at 200 kV. SERS experiments were recorded on a NOVA 2S-EX (325–1100 nm) Raman spectrometer under a 785 nm laser source excitation with 200 mW laser power (Ideal Optics, Shanghai, China). Optical microscopy images were captured on a BX53M microscope (Olympus, Japan).

Supporting Information Summary

The Supporting Information contains the test of the solubility of modified GNRs (THF, Chloroform and Toluene), TEM image of GNRs, Optical images of CTAB-capped GNRs in aqueous solution and MPS-ODS-capped GNRs in toluene solution, MPS and NaOH participate in the regulation of reaction quantity and the corresponding extinction spectra.

Acknowledgements

The authors thank Sudan Shen for her assistance in TEM at State Key Laboratory of Chemical Engineering (Zhejiang University). The authors also acknowledge financial support from National Natural Science Foundation of China (NSFC, Grant No. 61905056). This work was also supported by National Key R&D Program of China (Grant: 2018YFE0207500), the National Natural Science Foundation (Grant 91938201 and 61871169), Zhejiang Provincial Natural Science Foundation (Grant LZ20F010004) and Project of Ministry of Science and Technology (Grant D20011).

Conflict of Interests

The authors declare no conflict of interest.

Data Availability Statement

The data that support the findings of this study are available from the corresponding author upon reasonable request.

Keywords: gold nanorods · phase transfer · critical micelle concentration · self-assembly · surface enhanced Raman scattering

- [1] a) E. Alipour, D. Halverson, S. McWhirter, G. C. Walker, *Annu. Rev. Phys. Chem.* **2017**, *68*, 261–283; b) S. Burgess, A. Vishnyakov, C. Tsovko, A. V. Neimark, *J. Phys. Chem. Lett.* **2018**, *9*, 4872–4877; c) S. Burgess, Z. Wang, A. Vishnyakov, A. V. Neimark, *J. Colloid Interface Sci.* **2020**, *561*, 58–70; d) M. Das, U. Dahal, O. Mesele, D. Liang, Q. Cui, *J. Phys. Chem. B* **2019**, *123*, 10547–10561; e) A. J. Urquhart, A. Z. Eriksen, *Drug Discovery Today* **2019**, *24*, 1660–1668.
- [2] a) F. Gao, Y. Zhang, F. Ren, Y. Shiraiishi, Y. Du, *Adv. Funct. Mater.* **2020**, *30*, 2000255; b) F. Gao, Y. Zhang, H. You, Z. Li, B. Zou, Y. Du, *Small* **2021**, *17*, 2101428; c) Y. Gao, W. Nie, Q. Zhu, X. Wang, S. Wang, F. Fan, C. Li, *Angew. Chem. Int. Ed.* **2020**, *59*, 18218–18223; d) D. Lin, X. Zheng, X. Feng, N. Sheng, Z. Song, Y. Liu, X. Chen, Z. Cai, D. Chen, C. Yang, *Green Energy & Environ.* **2020**, *5*, 433–443; e) P. Prielcel, H. Adekunle Salami, R. H. Padilla, Z. Zhong, J. A. Lopez-Sanchez, *Chin. J. Catal.* **2016**, *37*, 1619–1650.
- [3] R. S. Sundaram, M. Steiner, H. Y. Chiu, M. Engel, A. A. Bol, R. Krupke, M. Burghard, K. Kern, P. Avouris, *Nano Lett.* **2011**, *11*, 3833–3837.
- [4] a) Y. Guo, Q. Zhou, X. Chen, Y. Fu, S. Lan, M. Zhu, Y. Du, *J. Mater. Sci. Technol.* **2022**, *119*, 53–60; b) D. B. Lioi, V. Varshney, S. Izor, G. Neher, W. J. Kennedy, *J. Mater. Chem. C* **2019**, *7*, 14471–14492; c) N. Zhang, C. Han, Y.-J. Xu, J. J. Foley IV, D. Zhang, J. Codrington, S. K. Gray, Y. Sun, *Nat. Photonics* **2016**, *10*, 473–482; d) A. Zhang, Y. Zhang, Z. Liu, G. Huang, L. Wu, Y. Fu, X. Wang, Y. Du, *Appl. Mater. Today* **2022**, *29*, 101575.
- [5] a) D. Ni, W. Bu, E. B. Ehlerding, W. Cai, J. Shi, *Chem. Soc. Rev.* **2017**, *46*, 7438–7468; b) R. M. Pallares, N. T. K. Thanh, X. Su, *Nanoscale* **2019**, *11*, 22152–22171; c) G. Russo, J. Witos, A. H. Rantamaki, S. K. Wiedmer, *BBA-Biomembranes* **2017**, *1859*, 2361–2372.
- [6] a) P. Biagioni, J. S. Huang, B. Hecht, *Rep. Prog. Phys.* **2012**, *75*, 024402; b) P. Zijlstra, J. W. Chon, M. Gu, *Nature* **2009**, *459*, 410–413; c) P. Zijlstra, M. Orrit, *Rep. Prog. Phys.* **2011**, *74*, 106401.
- [7] X. Dai, Z. Jiao, Z. Ma, K. Liu, C. Wang, H. Su, *J. Phys. Chem. C* **2019**, *123*, 20325–20332.
- [8] L. Song, N. Qiu, Y. Huang, Q. Cheng, Y. Yang, H. Lin, F. Su, T. Chen, *Adv. Opt. Mater.* **2020**, *8*, 1902082.
- [9] a) S. Maji, B. Cesur, Z. Zhang, B. G. De Geest, R. Hoogenboom, *Polym. Chem.* **2016**, *7*, 1705–1710; b) M. S. Strozyk, M. Chanana, I. Pastoriza-Santos, J. Pérez-Juste, L. M. Liz-Marzán, *Adv. Funct. Mater.* **2012**, *22*, 1436–1444.
- [10] a) J. Visser, *Adv. Colloid Interface Sci.* **1972**, *3*, 331–361; b) D. Jimenez de Aberasturi, A. B. Serrano-Montes, J. Langer, M. Henriksen-Lacey, W. J. Parak, L. M. Liz-Marzán, *Chem. Mater.* **2016**, *28*, 6779–6790.
- [11] a) M. Brust, M. Walker, D. Bethell, D. J. Schiffrin, R. Whyman, *J. Chem. Soc. Chem. Commun.* **1994**, *0*, 801–802; b) I. Ojea-Jime'nez, L. Garcia-Ferna'ndez, J. Lorenzo, V. F. Puentes, *ACS Nano* **2012**, *6*, 7692–7702.
- [12] a) Y. Lee, J. Jang, J. Yoon, J. W. Choi, I. Choi, T. Kang, *Chem. Commun.* **2019**, *55*, 3195–3198; b) A. M. Alkilany, A. I. B. Yaseen, J. Park, J. R. Eller, C. J. Murphy, *RSC Adv.* **2014**, *4*, 52676–52679.
- [13] a) S. Kittler, S. G. Hickey, T. Wolff, A. Eychmüller, *Z. Phys. Chem.* **2015**, *229*, 235–245; b) M. Lista, D. Z. Liu, P. Mulvaney, *Langmuir* **2014**, *30*, 1932–1938; c) Y. Wen, X. Jiang, G. Yin, J. Yin, *Chem. Commun.* **2009**, 6595–6597.
- [14] I. O.-J. nez, L. G. a.-F. ndez, J. Lorenzo, V. F. Puentes, *ACS Nano* **2012**, *6*(9), 7692–7702.
- [15] N. Yang, T. You, Y. Gao, S. Lu, P. Yin, *Langmuir* **2019**, *35*, 4626–4633.
- [16] M. A. A. Nahid, M. Karikomi, E. Nasuno, N. Kato, T. Sato, K. I. Iimura, *J. Oleo Sci.* **2022**, *71*, 685–692.
- [17] M. G. Soliman, B. Pelaz, W. J. Parak, P. del Pino, *Chem. Mater.* **2015**, *27*, 990–997.
- [18] Y. I. Derikov, G. A. Shandryuk, R. V. Talroze, A. A. Ezhov, Y. V. Kudryavtsev, *Beilstein J. Nanotechnol.* **2018**, *9*, 616–627.
- [19] a) J. Shan, H. Tenhu, *Chem. Commun.* **2007**, 4580–4598; b) R. A. Sperling, W. J. Parak, *Phil. Trans. R. Soc. A* **2010**, *368*, 1333–1383; c) Z. Zhang, S. Maji, A. B. d. F. Antunes, R. De Rycke, Q. Zhang, R. Hoogenboom, B. G. De Geest, *Chem. Mater.* **2013**, *25*, 4297–4303; d) W. Wei, G. Ge, *Part. Part. Syst. Charact.* **2013**, *30*, 837–841.
- [20] a) A. B. Serrano-Montes, D. Jimenez de Aberasturi, J. Langer, J. J. Giner-Casares, L. Scarabelli, A. Herrero, L. M. Liz-Marzán, *Langmuir* **2015**, *31*, 9205–9213; b) B. Tim, P. Błazkiewicz, A. B. Nowicka, M. Kotkowiak, *Appl. Surf. Sci.* **2022**, *573*, 151518.
- [21] M. Chanana, L. M. Liz-Marzán, *Nat. Photonics* **2012**, *1*, 199–220.
- [22] C. Kinnear, H. Dietsch, M. J. Clift, C. Endes, B. Rothen-Rutishauser, A. Petri-Fink, *Angew. Chem. Int. Ed.* **2013**, *52*, 1988–1992.
- [23] K. Mitamura, Toyoko Imae, N. Saito, O. Takai, *J. Phys. Chem. B* **2007**, *111*, 8.
- [24] a) X. Zhang, Z. Zhao, L. Liu, Y. Li, *Chem. Phys. Lett.* **2019**, *721*, 117–122; b) Z. Ye, C. Li, Q. Chen, Y. Xu, S. E. J. Bell, *Nanoscale* **2021**, *13*, 5937–5953.
- [25] S. S. Patel, K. Kumar, D. O. Shah, J. J. Delfino, *J. Colloid Interface Sci.* **1996**, *183*, 603–606.
- [26] M. L. Coluccio, G. Das, F. Mearini, F. Gentile, A. Pujia, L. Bava, R. Tallero, P. Candeloro, C. Liberale, F. De Angelis, E. Di Fabrizio, *Microelectron. Eng.* **2009**, *86*, 1085–1088.
- [27] a) M. Z. Wei, T. S. Deng, Q. Zhang, Z. Cheng, S. Li, *ACS Omega* **2021**, *6*, 9188–9195; b) X. Ye, C. Zheng, J. Chen, Y. Gao, C. B. Murray, *Nano Lett.* **2013**, *13*, 765–771.
- [28] Y.-J. Lee, N. B. Schade, L. Sun, J. A. Fan, D. R. Bae, M. M. Mariscal, G. Lee, F. Capasso, S. Sacanna, V. N. Manoharan, G.-R. Yi, *ACS Nano* **2013**, *7*, 11064–11070.

Manuscript received: March 19, 2023

ChemistrySelect

Supporting Information

Ethanol as a 'Catalyst' for Effective Phase Transfer and Self-Assembly of Gold Nanorods

Min Zhang, Tian-Song Deng,* and Zhiqun Cheng



Figure S1. Modified GNRs were dispersed in THF, chloroform and toluene at volume ratio of water / solvent =1:1.

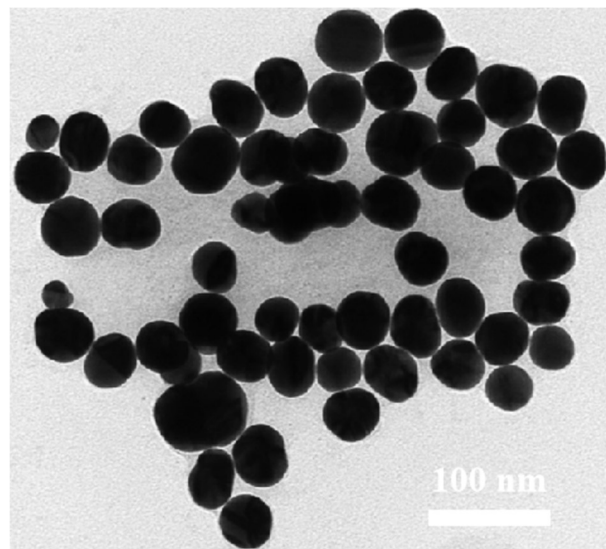


Figure S2. TEM image of CTAB-capped GNRs with the diameter of 66.1 ± 8.2 nm.

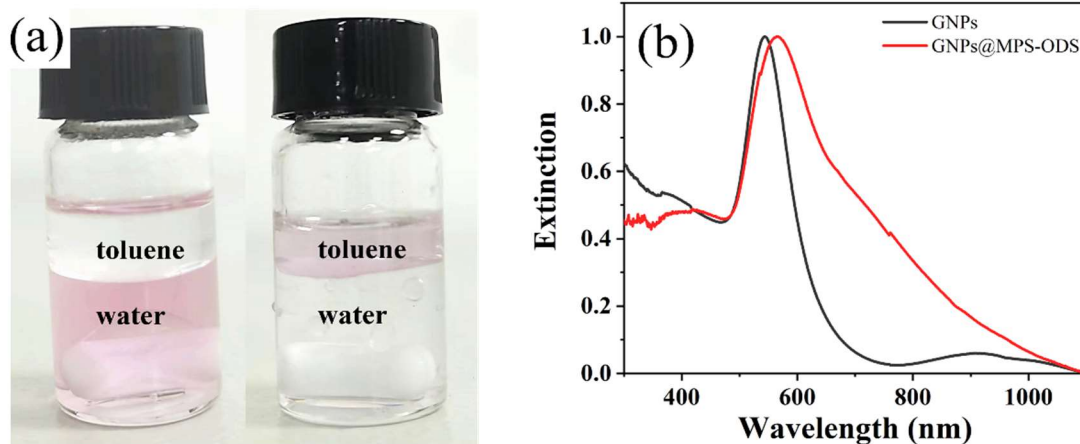


Figure S3. (a) Optical images of CTAB-capped GNPs in aqueous solution (left) and MPS-ODS-capped GNPs in toluene solution (right). (b) Extinction spectra of GNPs before and after ligand exchange.

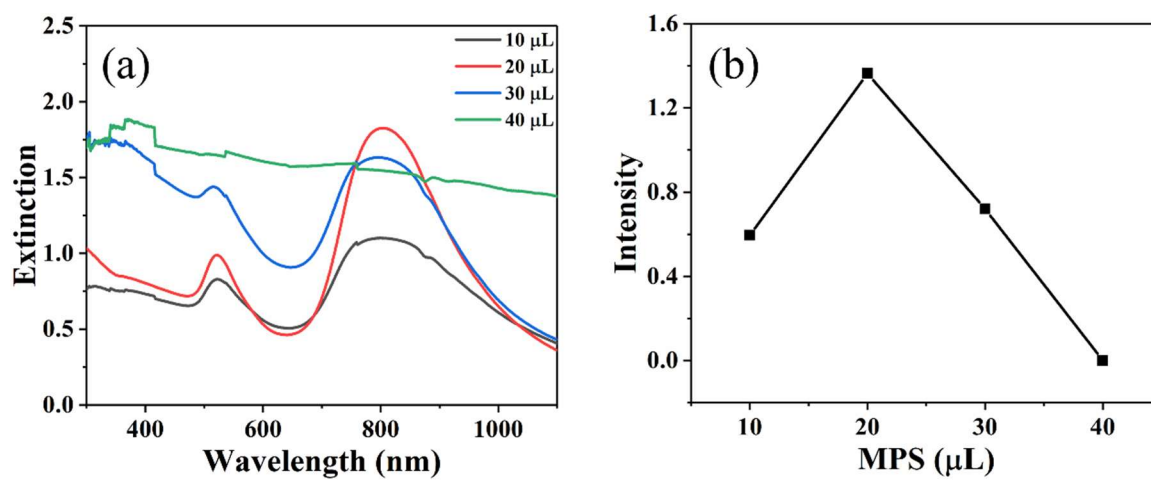


Figure S4. (a) Extinction spectra of different MPS contents and (b) extinction intensity of different MPS content.

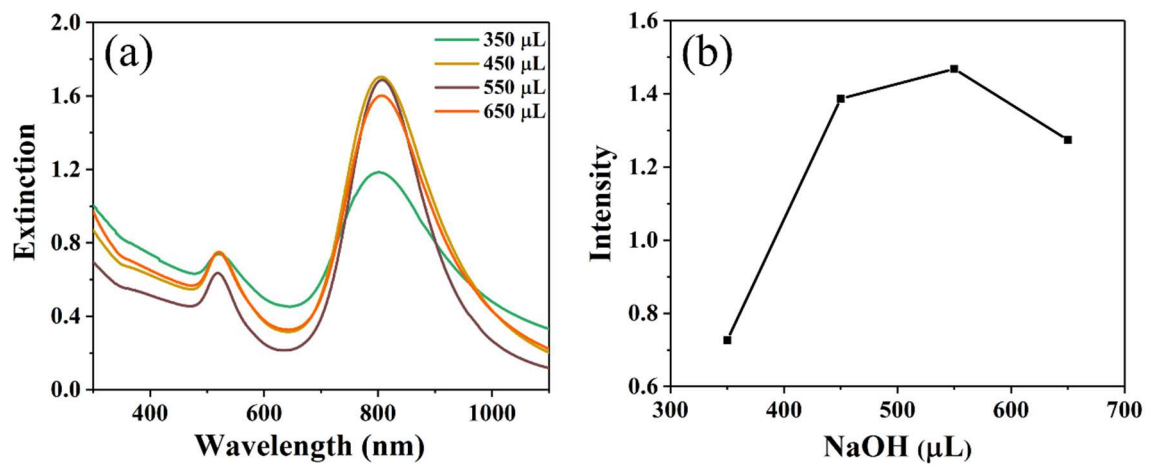


Figure S5. (a) Extinction spectra of different NaOH contents and (b) extinction intensity of different NaOH content.